Energy 282 (2023) 128781

Contents lists available at ScienceDirect

Energy

journal homepage: www.elsevier.com/locate/energy

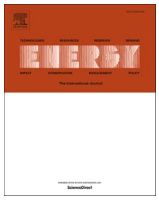

Voltage distribution analysis and non-uniformity assessment in a 100 cm^2 PEM fuel cell stack

G.M. Cabello González [a,*], Baltasar Toharias [a], Alfredo Iranzo [a,b], Christian Suárez [a,b], Felipe Rosa [a]

[a] Departamento de Ingeniería Energética, Grupo de Termotecnia. Escuela Técnica Superior de Ingeniería. Universidad de Sevilla. Camino de los Descubrimientos s/n. 41092, Sevilla, Spain

[b] AICIA - Grupo de Termotecnia. Camino de los Descubrimientos s/n. 41092, Sevilla, Spain

ARTICLE INFO

Handling editor: A. Olabi

Keywords:
fuel cell stack
Polymer electrolyte membrane stack
Operating conditions
Individual cell performance

ABSTRACT

In this study, a comprehensive set of experimental tests were carried out to investigate individual cell voltage and temperature deviation under different operating conditions in a fuel cell stack. Five key operating conditions were considered: temperature, pressure, anode and cathode relative humidity, and cathode stoichiometry. Different configurations of reactant flow within the stack were also investigated. A 100 cm^2 7-cell stack was used for the experiments, and voltage and temperature measurements were taken for each individual cell. Both ANOVA and range analysis method were used to evaluate the results. The findings showed that the performance of the external cells was consistently lower than that of the central ones since its temperature, the parameter that most affected performance, was also lower due to heat losses. Additionally, voltage deviation increased with temperature deviation. The study also revealed that stack performance was improved by an increase in temperature, pressure and cathode stoichiometry, whereas the effect of anode and cathode humidity was not so significant in the studied range. Furthermore, gravity played a clear role in water management, hindering the removal of condensed water for flow configurations where reactant gases were fed from the bottom interfaces of the stack.

1. Introduction

Nowadays, climate change is considered one of the most pressing environmental issues. The most recent study by the Intergovernmental Panel on Climate Change (IPCC) [1] unequivocally points the extensive use of fossil fuels by humans as the main cause of the planet's rising average temperature and the increasing occurrence of atypical atmospheric phenomena. As a result, there is a strong demand for clean power generation and, in this sense, fuel cells are a promising alternative to internal combustion engines. In recent years, fuel cells have gained exponential attention due to its competitive power density, high efficiency, quick start-up and load response, as well as low local emissions. The use of polymer electrolyte membrane (PEM) fuel cells for supplying energy in residences, transport and small-scale distributed generation systems requires that the fuel cell responds to a wide range of operating conditions in order to reach the optimal operating point.

To meet the power demand of practical applications such as transportation, cells are connected in series to form a stack, whose design and operating conditions need to be adjusted for improved performance and a longer lifetime. While there are several studies in the literature for the modeling and simulation [2–6], operating conditions optimization [7–9], water management [10–13], and membrane electrode assembly (MEA) durability of a single PEM fuel cell [14–16], the experimental study of stack has received less attention. However, stack behavior cannot be fully understood by analyzing the performance of a single cell, as non-uniformity in potential, temperature, and reactant and product flow distributions are observed in stacks [17]. Understanding how different operating conditions affect each individual cell is crucial, as relevant issues such as the operating life of stacks are subject to the performance of its worst single cell. Therefore, voltage and temperature uniformity are desirable [18].

Gas pressure, mass flow rate, temperature, reactant gas stoichiometry, humidity, and heat management [17] are all factors that can impact the voltage uniformity of a PEM fuel cell. Studies have found that an increase in current density can lead to a higher voltage deviation due to increased water production and channel flooding [19,20]. On the

* Corresponding author.
E-mail address: gcabello3@us.es (G.M. Cabello González).

https://doi.org/10.1016/j.energy.2023.128781
Received 15 December 2022; Received in revised form 24 July 2023; Accepted 14 August 2023
Available online 18 August 2023

other hand, an increase in fuel humidity can lead to a higher voltage deviation due to a drop in internal cell resistance [21]. Also, voltage distribution is more homogeneous at higher temperatures due to an increase in the membrane conductivity and at higher flow rates that provide a more even gas distribution [22,23]. Dynamic load experiments with PEM fuel cell stacks [24] have shown that cell voltage uniformity can be disturbed during a fast dynamic response process, as liquid water in the diffusion layer can cause differences in diffusion coefficients between single cells, leading to uneven oxygen concentrations across the catalyst surfaces. Adjusting the amplitude of the current step and the frequency of current variation can help mitigate these changes in voltage uniformity. Thermal management on fuel cell stacks is also a key concern, especially in compact designs, due to the problem of heat dissipation, as temperature gradients can severely impact performance [25,26]. Innovative solutions, such as micro heat pipes, have been tested to ensure thermal homogeneity [27].

Regarding how operating conditions affect fuel cell performance, Iranzo et al. [8] found that, for a 50 cm^2 parallel-serpentine PEM fuel cell, increasing the cell temperature from 55 °C to 75 °C reduced cell performance, and that this effect was more pronounced at higher current densities. Also, increasing the reactant relative humidity and cell backpressure had a positive effect on the cell performance. Finally, the cell performance slightly improved at high cathode stoichiometric factors, being this enhancement only significant at high current densities as more gas flow provided a high water removal capability. Recently, Saka et al. [9] investigated the influence of operating conditions on a 100 cm^2 single PEM fuel cell equipped with a Nafion HP membrane. They observed that an operating temperature around 65 °C allowed quick start-up and enhanced power density, since less thermal insulation was required. However, at higher temperatures, the tolerance of the fuel cell to impurities was enhanced, and also humidity control and water management were improved. Additionally, increasing the operating pressure had a positive effect on cell efficiency. Besides, cathode stoichiometry had a more significant impact on cell performance than anode stoichiometry, with higher oxygen flows being desirable, as they provided high oxygen concentration and helped remove the excess of water at high current densities. An innovative study carried out by Suárez et al. [28] over a 50 cm^2 bioinspired PEM fuel cell showed that decreasing the cell temperature from 75 to 55 °C had a positive effect on cell performance. In addition, an increase in cell back pressure and relative humidity of the anode and cathode streams improved cell performance. A thorough design of experiments and parameter optimization was carried out by Xia et al. [29], showing interesting results of practical value when optimizing operating cell fuel parameters. They found, for a 250 cm^2 active area fuel cell, that the influence of the different parameters (temperature, inlet pressure, gas relative humidity, and oxidant stoichiometric ratio) on cell performance varied with current density. That way, the effect of the air stoichiometric ratio was largest for medium and high current density, while gas inlet pressure was most noticeable at low current density. On the other hand, operating temperature and reactant relative humidity had a non-obvious impact on cell performance. In summary, when testing single fuel cells, it is commonly observed that temperature hinders performance as membrane dry out rises, limiting its conductivity. Also, pressure has a positive effect on the polarization curve, as the partial pressure of hydrogen and oxygen increases, favoring the contact of the gases with the electrolyte and, therefore, the rate of the chemical reaction. Reactant humidity also impacts on the cell performance, increasing its efficiency if proper water management is given, as it humidifies the membrane, preventing it from drying out. Finally, cathode stoichiometry has a significant influence as it provides higher oxygen concentration and prevents water flooding, whether a higher anode stoichiometry has a minimal impact on cell performance.

Some investigations have been published analyzing how different parameters affect PEM fuel cell stacks. In a study conducted by Jang et al. [21], experiments were carried out on a 5-cell stack with a distribution area of 10x10 cm^2. The authors found that the stack performance increased as the temperature rose, with the end cells (cells 1 and 5) presenting higher voltage than the central ones and a higher voltage dispersion at higher temperatures. Humidification of the anode and cathode flow was also found to benefit the stack operation, as water management improved, especially for the central cells. On the other hand, the anode gas stoichiometric ratio had little effect on the stack performance, while a higher cathode gas stoichiometric ratio improved the stack performance and resulted in a more homogeneous voltage distribution. More recently, Costa et al. [30] found that, working with a 1 kW PEM fuel cell stack, a rise in operating temperature caused poorer stack performance and wider variation in individual cell voltages, which they attributed to deficient water distribution. They also found that the optimal air stoichiometry was 2, as for a stoichiometry of 1.5 channels flooded and, for a stoichiometry of 3, membrane dehydration decreased stack performance.

From the above literature review, it is clear that the majority of prior research has investigated the effect of operating conditions on the performance of single fuel cells, but less attention has been paid to fuel cell stacks. Furthermore, the studies found over a complete stack do not necessarily present similar results to the behavior of a single PEM fuel cell and mainly focus on the average cell voltage, not considering the cell voltage distribution. Hence, the literature lacks of investigations over fuel cell aggregations that better represent the performance of an industrial stack. The aim of this paper is to investigate the performance of a 500 W PEM stack at different operating conditions, not only as a whole, but also by observing each cell individually. The novelty and main contributions of this work are highlighted in the following bullet points.

- The experiments were carried out with a 7-cell 100 cm^2 active area PEM fuel cell stack. Since most experimental studies found in the literature only test a single cell, and it has been proven that the behavior of a stack is different, this study presents results closer to a commercial solution.
- The study includes a greater number of stack operating variables compared to previous works identified in the literature, making it a highly valuable contribution to the field. By incorporating a broader range of stack operating variables, the research expands the scope of analysis and enhances our understanding of the system's behavior. This comprehensive approach enables a more nuanced examination, providing deeper insights and paving the way for advancements in the field of stack operations.
- Due to the fact that voltage distribution is a key parameter to evaluate system performance, health state and reliability; not only has the average cell voltage performance been assessed, but also the performance of each individual cell, taking measures of individual voltages and temperatures.
- Two statistical studies, the Analysis of Variance (ANOVA) and the range analysis method, have been conducted to examine how different operating conditions affect both the average stack voltage and the voltage dispersion. The study goes beyond the typical analysis found in the literature, providing a more in-depth examination. By utilizing both methods, clear trends and the relative importance of the variables studied have been identified.
- Also, a study on how flow configuration affects stack performance was carried out for the four possible options, assessing IV curves and voltage and temperature heterogeneity.

To the best of the author's knowledge, there is no study in the literature that assesses altogether these aspects within a PEM fuel cell stack. This work is structured as follows. First, a brief introduction places the reader in the PEM fuel cell stack context and explains the goal and innovation of the study. After that, the methodology is presented, including a description of the test bench as well as the 500W stack used for the different experiments. The paper then includes an analysis of the results obtained during the tests. Finally, the document ends with a brief

conclusion section.

2. Experimental facility and methodology

2.1. Experimental setup. Test bench and stack description

The tested device was a PEM fuel stack composed of 7-cells with an active area of 100 cm^2, supplied by Pragma Industries, as shown in Fig. 1. Each cell was made up of two bipolar plates (an anode and a cathode) that, when assembled, form an internal cooling circuit that was refrigerated with deionized water. The bipolar plates had a serpentine design flow field with a channel to rib ratio of 1, being the width of the channel and the rib 1 mm each, and the total thickness of each plate 6 mm. The recommended flow distribution by the manufacturer is shown in Fig. 2. A 7-layer Membrane Electrode Assembly (MEA) with an active area of 100 cm^2 and 0.4 mg Pt/cm^2 on both anode and cathode electrodes was used.

The experimental work was conducted using a dedicated PEM fuel cell station for testing PEM single cells and short stacks up to 500 W. The test environment included a reagent gas handling unit, which consisted of mass flow controllers, humidifiers, temperature control system, back pressure regulators, and an electronic load. Additionally, the bench incorporated two systems for temperature regulation of the cell/stack. The first system was a PID-controlled cell heating/cooling system based on deionized water as the heat transfer fluid, while the second system used air fans for small cells without the option of liquid refrigeration. To ensure optimal conditions in the stack, temperature and pressure in the inlet/outlet lines were monitored at several points. Individual voltage and temperature were measured for each cell. A sketch of the P&ID from the control panel is shown in the work of Suárez et al. [28].

2.2. Operating conditions and experimental testing procedure

A wide range of operating conditions were used to analyze their effect on fuel cell performance. The nomenclature used to identify the tests is as follows: **P**AA_**T**BB_**a**CC**HR**DD_**c**EE**HR**FF**air**, where AA represents the operating pressure in bar with a decimal, BB represents the operating temperature in Celsius, CC represents the anode stoichiometry with a decimal, DD represents the anode relative humidity in %, EE represents the cathode stoichiometry with a decimal, and FF represents the cathode relative humidity in %. The word "air" is indicated at the end to show that the experiment was carried out feeding air instead of pure oxygen in the cathode. Therefore, the experiment named P10_T70_a15HR60_c30HR55air corresponds to a test carried out at P = 1.0 bar, T = 70 °C, λa = 1.5, RHa = 60%, λc = 3.0, and RHc = 55%. Table 1 summarizes all the test carried out, where the variation for each operating condition with respect to the first essay is marked in bold. A total of 18 operating conditions were tested, varying temperature (60, 70, 80 °C), pressure (0.5, 1.0, 1.5 bar), anode relative humidity (50, 60, 70%), cathode relative humidity (45, 55, 65%), and cathode stoichiometry (1.5, 2.0, 3.0). For every test, the anode stoichiometry was set in 1.5, and air was used as the oxidizing reagent.

In order to study the influence of the reactant gas position (top to bottom or vice versa), four extra tests were carried out at P = 1.0 bar, T = 80 °C, λa = 1.5, RHa = 60%, λc = 2.5, and RHc = 55%, testing the four possible configurations of the inlet/outlet hoses: anode and cathode gas inlet at the top with gas outlet at the bottom, cathode gas inlet at the bottom with gas outlet at the top, anode gas inlet at the bottom with gas outlet at the top, and anode and cathode gas inlet at the bottom with gas outlet at the top.

The I–V polarization curves for the fuel cell stack were obtained following the next experimental methodology. The tests began with membrane activation, as described in the user guide provided by Pragma Industries. The fuel cell stack was operated for 24 h in activation conditions, which were atmospheric pressure, cell temperature of 65 °C, relative humidity of anode and cathode of 100%, and a stoichiometric factor of 1.5 and 3 for the anode and cathode, respectively. When these conditions were achieved, current density was progressively increased until the voltage indicated on the test bench was 0.6 V per cell.

Once the membrane was activated, the tests were performed setting the different conditions specified in Table 1. The testing methodology was defined in FCTESTNET [31] and FCTESTQA [32]. First, the cell was preconditioned by setting the operating conditions to the specified values. To stabilize the conditions, the current density was gradually increased in steps of 0.1 A/cm^2 until a voltage of 0.5 V was achieved. Once this condition was reached, the current density was maintained for a period of 900 s to stabilize the operating conditions. Next, the cell was driven to Open Circuit Voltage (OCV) conditions for a period of 120 s. The measurement of these curves was performed in galvanostatic mode, starting from the OCV voltage and using fixed current density steps. For low current densities, periods of 120 s were used (i.e. from OCV up to a current density of 0.08 A/cm^2); while for higher current densities, the time period used was 300 s (i.e. from a current density of 0.1 A/cm^2 to the maximum current density that can be reached for each operating condition). The test finished when the voltage of one of the cells dropped under 0.3 V. The data acquisition rate of the test bench was 1 s, so the average value of the last 30 samples was used for post-processing of the data. In order to check the reproducibility of the results, tests with a cathode stoichiometry of 3 were replicated, and the average result is shown in the images.

In order to measure the dispersion of the individual voltages of every independent cell, the parameter C_v was defined as:

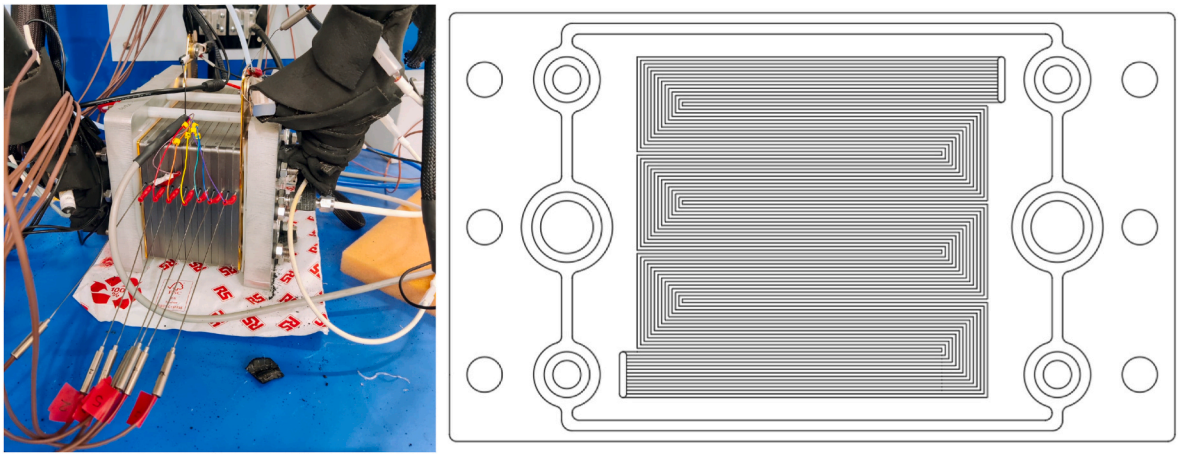

Fig. 1. Pragma industries' 7-cell stack used in the tests (left) and image of the plate design (right).

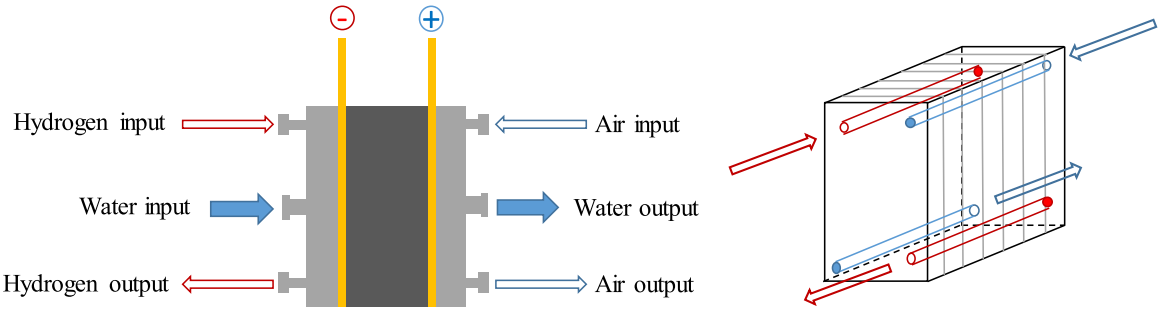

Fig. 2. Flow configuration for the 7-cell stack used in the tests. Front view (left) and perspective.

Table 1
Operating conditions defined in the experimental tests.

Case	P (bar)	T (°C)	RHa (%)	RHc (%)	λ_a (−)	λ_c (−)	oxidant
P10_T70_a15HR60_c30HR55air	1.0	70	60	55	1.5	3.0	air
P10_T60_a15HR60_c30HR55air	1.0	**60**	60	55	1.5	3.0	air
P10_T80_a15HR60_c30HR55air	1.0	**80**	60	55	1.5	3.0	air
P05_T70_a15HR60_c30HR55air	**0.5**	70	60	55	1.5	3.0	air
P15_T70_a15HR60_c30HR55air	**1.5**	70	60	55	1.5	3.0	air
P10_T70_a15HR70_c30HR55air	1.0	70	**70**	55	1.5	3.0	air
P10_T70_a15HR50_c30HR55air	1.0	70	**50**	55	1.5	3.0	air
P10_T70_a15HR60_c30HR45air	1.0	70	60	**45**	1.5	3.0	air
P10_T70_a15HR60_c30HR65air	1.0	70	60	**65**	1.5	3.0	air
P10_T70_a15HR60_c20HR55air	1.0	70	60	55	1.5	**2.0**	air
P10_T60_a15HR60_c20HR55air	1.0	**60**	60	55	1.5	**2.0**	air
P10_T80_a15HR60_c20HR55air	1.0	**80**	60	55	1.5	**2.0**	air
P05_T70_a15HR60_c20HR55air	**0.5**	70	60	55	1.5	**2.0**	air
P15_T70_a15HR60_c20HR55air	**1.5**	70	60	55	1.5	**2.0**	air
P10_T70_a15HR70_c20HR55air	1.0	70	**70**	55	1.5	**2.0**	air
P10_T70_a15HR50_c20HR55air	1.0	70	**50**	55	1.5	**2.0**	air
P10_T70_a15HR60_c20HR45air	1.0	70	60	**45**	1.5	**2.0**	air
P10_T70_a15HR60_c20HR65air	1.0	70	60	**65**	1.5	**2.0**	air

$$C_V = \frac{\sqrt{\frac{1}{N}\sum_{i=1}^{N}(V_i - \overline{V})^2}}{\overline{V}} \bullet 100 \quad (1)$$

where V_i is the voltage of individual cells, $\overline{V}$ the average voltage of the individual cell and N is the number of individual cells. That way, a high value of C_v indicates a bigger dispersion in the individual cell voltages and, consequently, a worse uniformity. To obtain the temperature dispersion, the parameter C_T was calculated using Equation (1) but considering temperature instead of voltage.

To analyze the experimental results, we utilized the range analysis method to assess the impact of the examined factors at different current density conditions [33,34]. This analysis encompassed both the average cell voltage and the voltage dispersion (C_v). Range analysis enabled us to evaluate the comparative sensitivity of factors based on the experimental outcomes, as defined by $R = \max(K_{ij}) - \min(K_{ij})$. Here, K_{ij} represents the factor i from Table 2 and the corresponding level j ranging from 1 to 3. K_{ij} was calculated using the experimental results of all test cases involving factor i at level j. The larger the range, the greater the sensitivity of the factor. Additionally, an Analysis of Variance (ANOVA) study was conducted with the software Statgraphics© using the 216 experimental data points, which included the average voltage and voltage dispersion for each operating condition at every current density. Furthermore, the same analysis was performed separately for the maximum and minimum considered current densities, allowing for a comparison of the results with those obtained from the range analysis method.

3. Results and discussion

3.1. Analysis of the operating conditions effect over the cell performance

Fig. 3 provides a summary of the results obtained from the 500 W stack. The individual voltage distribution with all the data from the different experiments can be found in Fig. S4 in the Supplementary Material file. Fig. 3 (top) shows the variation of the average cell voltage and C_v at low current densities (0.06 A/cm^2) with temperature, pressure, anode gas relative humidity, and cathode gas relative humidity for the two considered cathode stoichiometries. Fig. 3 (bottom) represents the same test results, but at higher current densities (1 A/cm^2). For the sake of simplicity, only the polarization curves at cathode stoichiometry of 3 are shown in Fig. 5, as the tendencies are the same at cathode stoichiometry of 2.

The results of the ANOVA study (Fig. S1) indicate that stack temperature has the greatest impact on the fuel cell stack performance, followed by cathode stoichiometry and pressure, while the effect of anode and cathode humidity is not statistically significant. As shown in Figs. 4 and 5 (bottom), the average cell voltage increases while increasing temperature at both low and high currents. This rise is of about 0.07 V for every 10 °C at 1 A/cm^2. This trend contradicts what was found in the literature and tested by the authors in single cells [8] or stacks [30], but agrees with a study carried out Jang et al. [21] over a 5 cells stack with a distribution area of 100 cm^2. This suggests that the behavior of an individual cell cannot be so easily extrapolated to a full stack as they may have different behaviors according to their design. Additionally, the variation of individual cell voltages increases at low

Table 2
Factors and their corresponding levels.

Case	L1	L2	L3
P (bar)	0.5	1	1.5
T (°C)	60	70	80
RHa (%)	50	60	70
RHc (%)	45	55	65
λ_c (−)	2	–	3

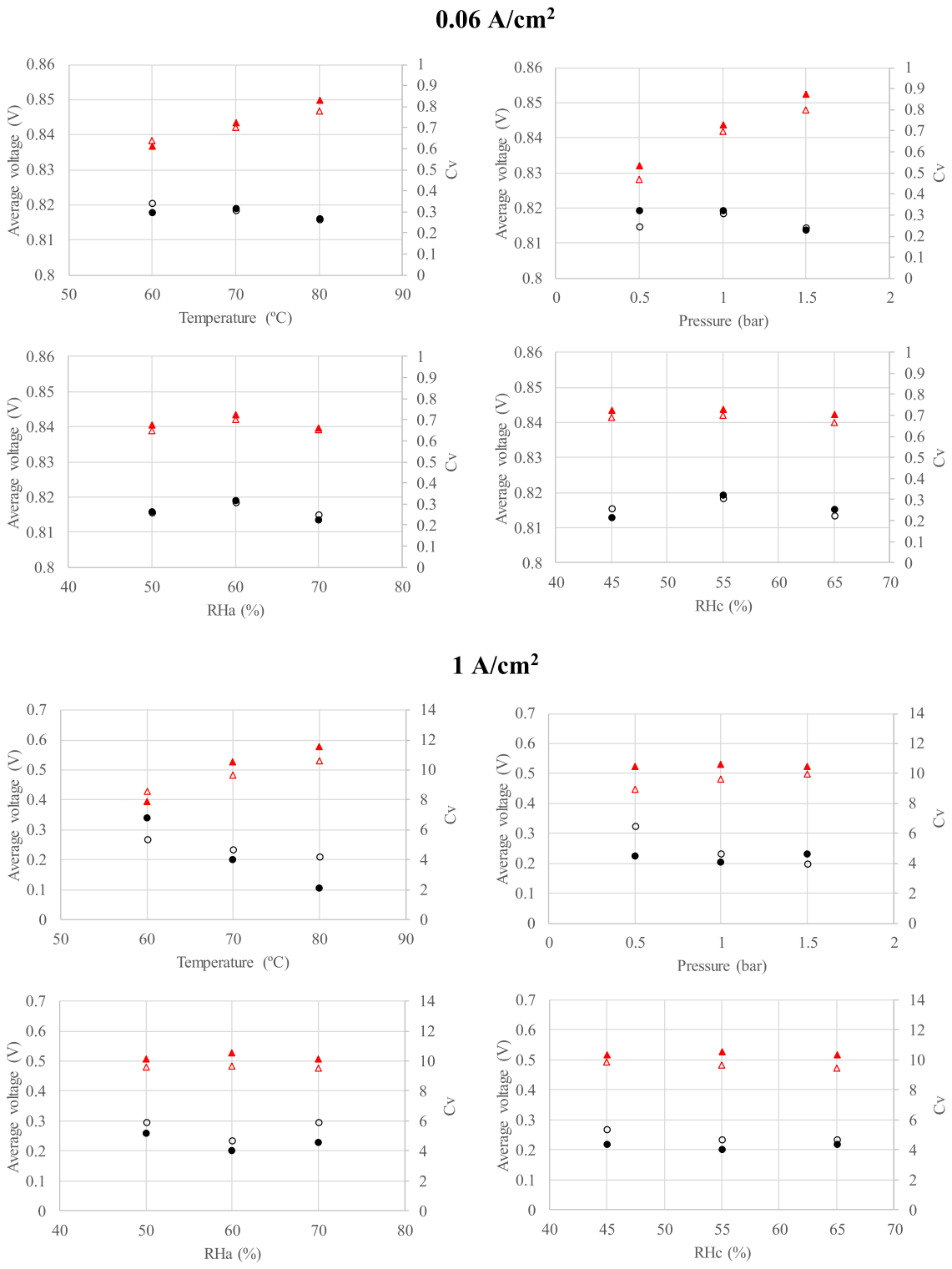

Fig. 3. Average voltage variation with the operating condition for a current density of (top) 0.06 A/cm^2 and (bottom) 1 A/cm^2. Δ average voltage (empty λc = 2, full λc = 3), ● C_v (empty λc = 2, full λc = 3).

temperatures, varying around 1.5 points each 10 °C at 1 A/cm^2. This effect may be attributed to the formation of water condensation slugs in the flow channels, causing an uneven pressure distribution in the stack cells and an irregular flow distribution, leading to uneven individual cell voltage.

An increase in stack pressure slightly improves cell performance at any current density. This effect is particularly noticeable at high current densities for the lowest cathode stoichiometry, increasing voltage by 0.03 V for each 0.5 bar at 1 A/cm^2. This improvement is due to the fact that activation and mass transport losses are reduced, as previously reported [8,28]. At high current density and high cathode stoichiometry, the effect of pressure is barely noticeable, increasing voltage only by 0.007 V for each 0.5 bar at 1 A/cm^2, since there is an abundant supply of oxygen. The relative humidity of the inlet gases barely affects the cell

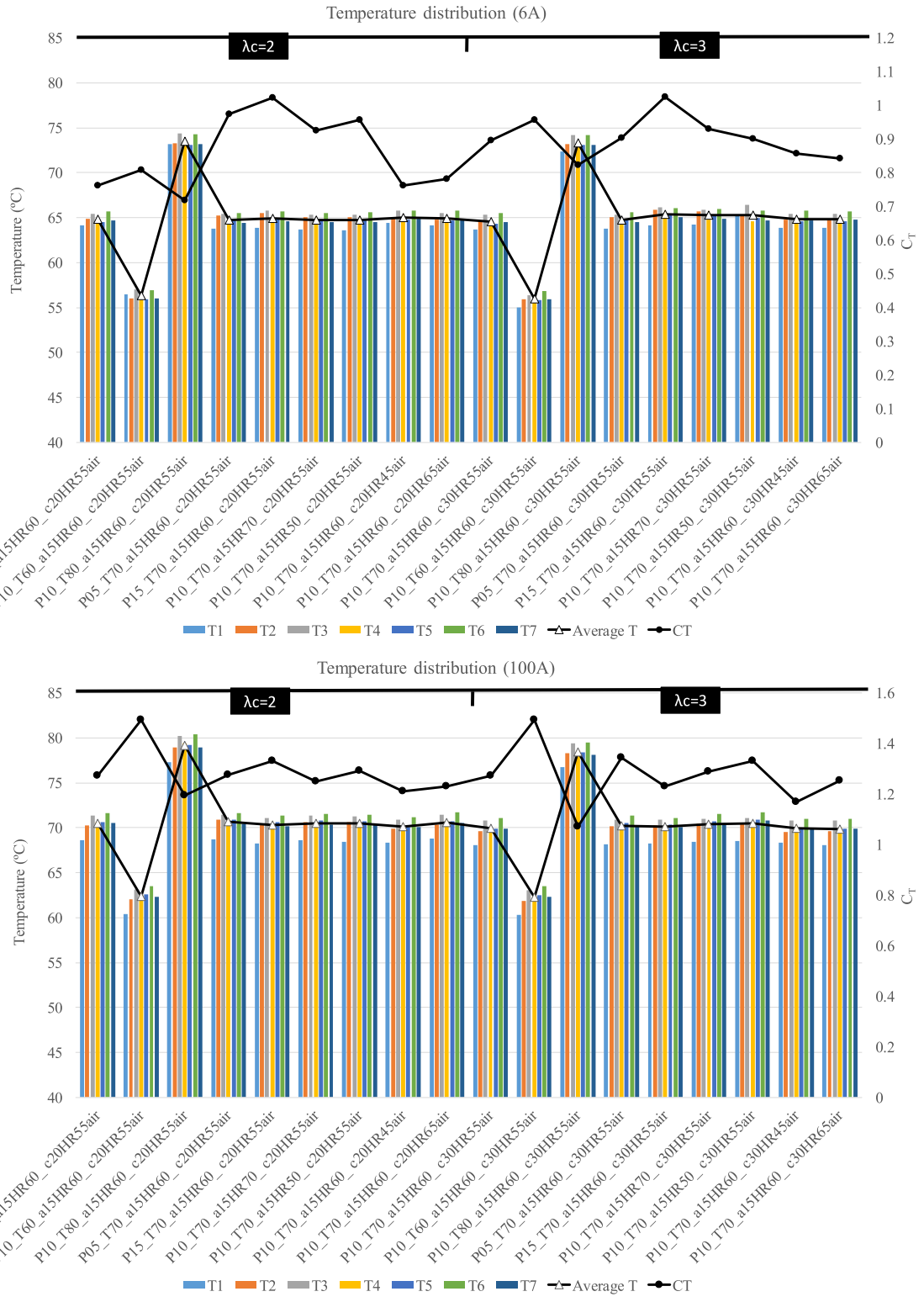

Fig. 4. Temperature distribution at a current density of 0.06 (top) and 1 A/cm^2 (bottom).

performance, although average humidities of 60% for the anode and 55% for the cathode side slightly improve cell operation.

Finally, switching from a cathode stoichiometry of 2–3 notably improves stack operation under any operating condition. This increase in the stack performance is greater at higher current densities, increasing by an average of 0.04 V at 1 A/cm^2 compared to 0.002 V at 0.06 A/cm^2, as higher stoichiometry implies higher oxygen flows, which allows for greater elimination of the water generated and accumulated in the cell channels. This, in turn, enables better distribution of oxygen flow throughout the specific surface in all the individual cells. This effect has been widely reported in the literature, not only for individual cells [8], but also for stacks [21]. However, this parameter also has an optimal operating range because if the gas flow is too high, membrane dehydration will decrease stack performance, as reported by Costa et al. [30].

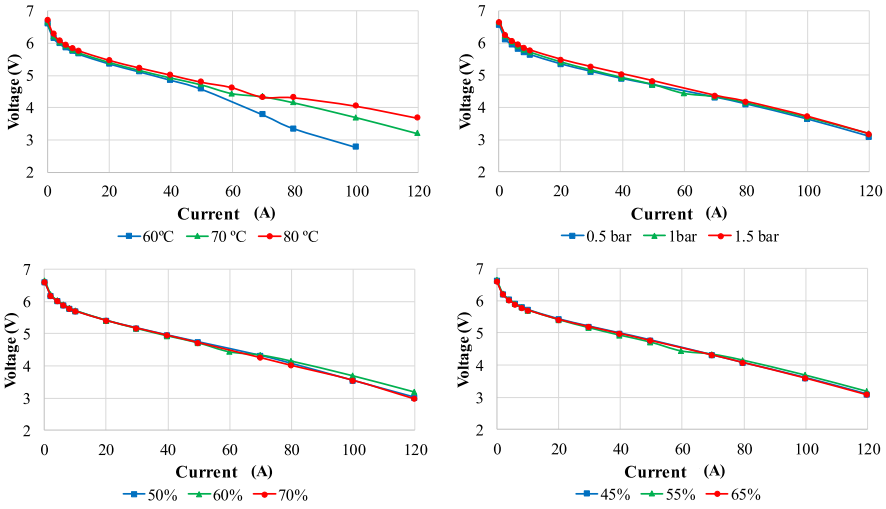

Fig. 5. Polarization curves for the block of experiments carried out with a cathode stoichiometry of 3. Variation with temperature (top left), pressure (top right), anode relative humidity (bottom left), and cathode relative humidity (bottom right).

Nonetheless, this improved gas distribution and water managements is reflected in a lower dispersion in individual voltages, decreasing C_v between 0.6 and 2 at 1 A/cm^2.

Average stack voltage was calculated for each operating condition and current density. The results (Fig. 6) indicated that pressure was the dominant factor for current densities below 0.4 A/cm^2, while temperature became dominant above that value. Graphic results of the range tests carried out for individual cells are shown in Fig. S5 in the Supplementary Material. ANOVA studies were conducted for extreme current densities, 0.04 and 2 A/cm^2 (Figs. S2 and S3), confirming this trend. At lower intensities, kinetics predominantly influenced the stack performance, so higher pressures will enhance the kinetics affecting the overall performance of the cell. At high current densities, increased temperature improved water management by promoting water evaporation and preventing excessive liquid water accumulation in the membrane. Moreover, the rate of electrochemical reactions was temperature-dependent, resulting in increased reaction rates and faster electrochemical processes at higher temperatures. Additionally, temperature affected the proton conductivity of the electrolyte membrane, facilitating faster ion transport.

The previous analysis was carried out considering average cell voltage but, voltage heterogeneity is crucial for maximizing efficiency, power output, and lifespan, preventing cell degradation and reversal, and enabling effective control and diagnostics. That way, the parameter C_v was calculated for every condition and a range analysis was carried out. Fig. 7 shows that temperature was the parameter that dominated voltage distribution at every current density. The importance of pressure at low current densities was reported by Su et al. [35] in a study carried out with a 140-cell PEM stack, where it was shown that the uniformity of a stack voltage distribution at low load current was improved increasing operating pressure. This result concurs with the data that was obtained while considering the average voltage in Fig. 6 but, in the present study, pressure has a non-significant role in voltage distribution. However, this is not a contrary result since Su et al. [35] only varied pressure, not considering changes in temperature or other factors.

It is clear that voltage uniformity diminishes as the current density increases (Fig. 3). For example, the average C_v value for all tests at 0.06 A/cm^2 was 0.3, while at 1 A/cm^2 was 4.8, indicating that the voltage distribution was 16 times less uniform at high current densities. This effect was also observed by Chen et al. [18] for a 6.55 kW PEM fuel cell stack used in transportation applications. They found that, in a dynamic driving cycle, voltage uniformity worsened with the increase of loading current and that there were some local maxima of C_v when step loading or unloading occurred. This effect may be due to the preferential

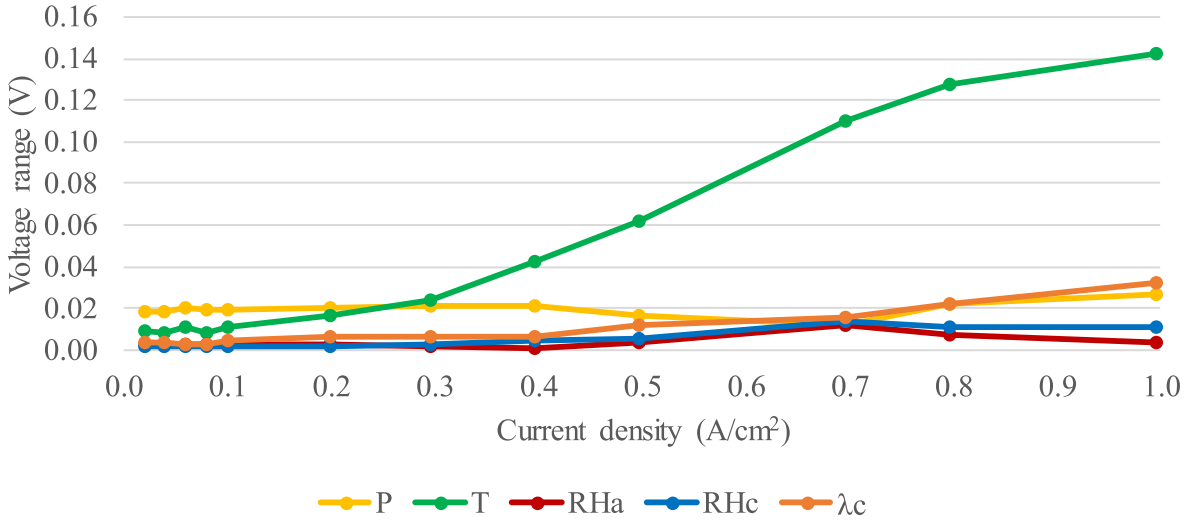

Fig. 6. Evolution of parameter relevance with current density for the stack average voltage. Range analysis method results.

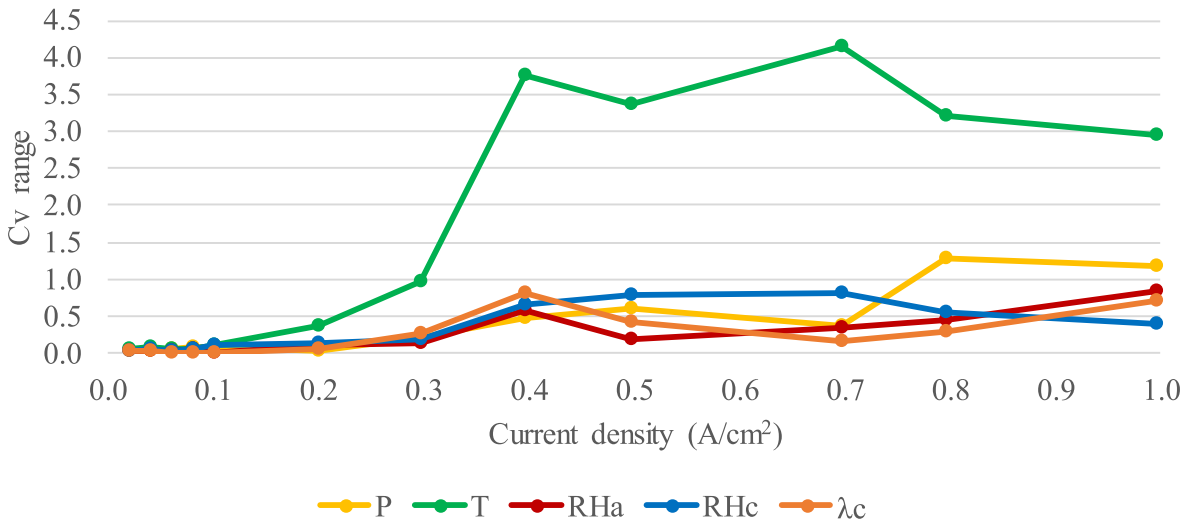

Fig. 7. Evolution of parameter relevance with current density for the stack voltage dispersion. Range analysis method results.

accumulation of water on some cells, altering gas distribution and reactant access to the catalyst active sites, which hinders the performance of some cells as concluded by Pérez-Page et al. [36]. This can also be caused by the fact that the decrease in hydrogen concentration leads to a decrease in the voltage consistency as reported by Chen et al. [37]. As can be seen, for every test, the cells at the ends of the stack have a lower voltage than the central ones. This result contradicts the findings of Jang et al. [21] in a 100 cm^2 5-cell stack with a triple channel serpentine design, as they observed that the end cells had a higher voltage than the central ones, because the center cell was less humidified. In our particular case, the cell voltage distribution followed the same trend as individual cell temperatures (Fig. 4). The same stack temperature distribution can be found in the work of Salva et al. [38] for different number of cell stacks. Consequently, as the non-uniformity of the temperature profile increases, the non-uniformity of the voltage profile also increases, and thus, the C_v associated to the voltage distribution rises with the increasing C_T related to the temperature distribution (Fig. 8). The research conducted by Mennola et al. [39] and Adzakpa et al. [40] revealed that as current densities increased, the temperature distribution within the stack became more uneven. This uneven distribution caused higher temperatures at the center compared to the ends, resulting in voltage differences between cells. As mentioned earlier, the temperature in the studied range significantly favored cell performance. Therefore, cells with a higher temperature exhibited a higher voltage. This irregular temperature distribution was a consequence of the uneven heat losses in the stack.

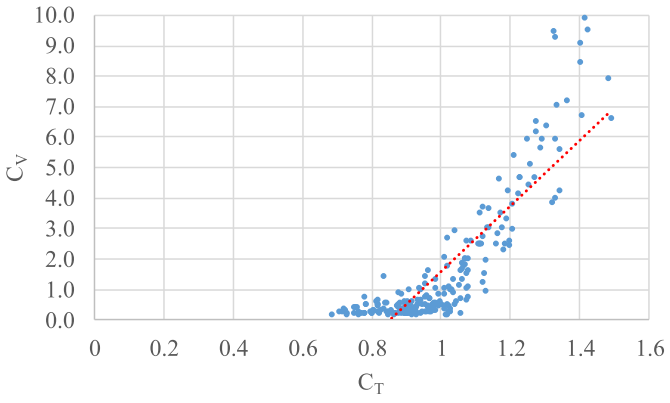

Fig. 8. Voltage distribution vs. temperature distribution.

3.2. Outcome of changes in the flow configuration

The flow configuration played a significant role in determining the performance of a Proton Exchange Membrane (PEM) fuel cell stack. It affected various aspects such as reactant distribution, mass transport, and overall cell efficiency. To study it, four tests were carried out under the same operating conditions (P = 1.0 bar, T = 80 °C, λa = 1.5, RHa = 70%, λc = 2.5, RHc = 55%) to observe how changes in the reactant inlet/outlet affect the stack performance. The different configurations tested are shown in Fig. 9, while the polarization curves for this group of experiments are presented in Fig. 10. Fig. S6 in the Supplementary Material presents the individual cell voltages. The nomenclature used to identify these experiments was *a* for anode, *c* for cathode, *b* for bottom and *t* for top. That way, the standard configuration was referred to as *atct*.

As can be observed, if both anode and cathode gases are fed from the bottom part of the stack (*abcb*), the stack performance is severely affected. At a medium current density (0.4 A/cm^2) the voltage of the first cell (the one closest to the anode side) drops abruptly below 0.3 V. The same occurs if the anode is fed from the bottom and the cathode from the top. On the other hand, if the cathode is fed from the bottom and anode from the top (*atcb*), the stack performs similarly to the *atct* configuration. Surprisingly, the *atcb* configuration performs better than the *atct* configuration at high current densities, reaching about 0.2 V more at 1 A/cm^2. From the results obtained it is clear that feeding the anode from the bottom part of the stack is dramatically affecting the voltage of the first cell and consequently of the whole stack (Fig. S6) and this flow configuration should be avoided. The first cell is becoming flooded and hydrogen tends to flow through the other cells in the stack, leaving the first cell with a very low feed of hydrogen and causing thus a dramatic decay in the cell voltage.

In the reference configuration, both gas inlets are in the top part of the stack, while the outlets are set at the bottom, so the gases circulate mainly countercurrent in the horizontal part of the serpentine but isocurrent or cross current in the vertical parts of the serpentine. This flow configuration presents a uniform reactant distribution, avoiding localized fuel starvation. Feeding the gases from the bottom part of the stacks hinders water management, as gravity does not help to evacuate liquid water slugs, especially in the exterior cells with lower temperature and consequently higher water condensation rates and possible flooding. This effect only affects the anode side because it has less gas flow and, therefore, less water carrying capacity. That way, the anode side presents flooded channels with an uneven pressure drop and gas distribution that negatively impact the stack's performance. On the other hand,

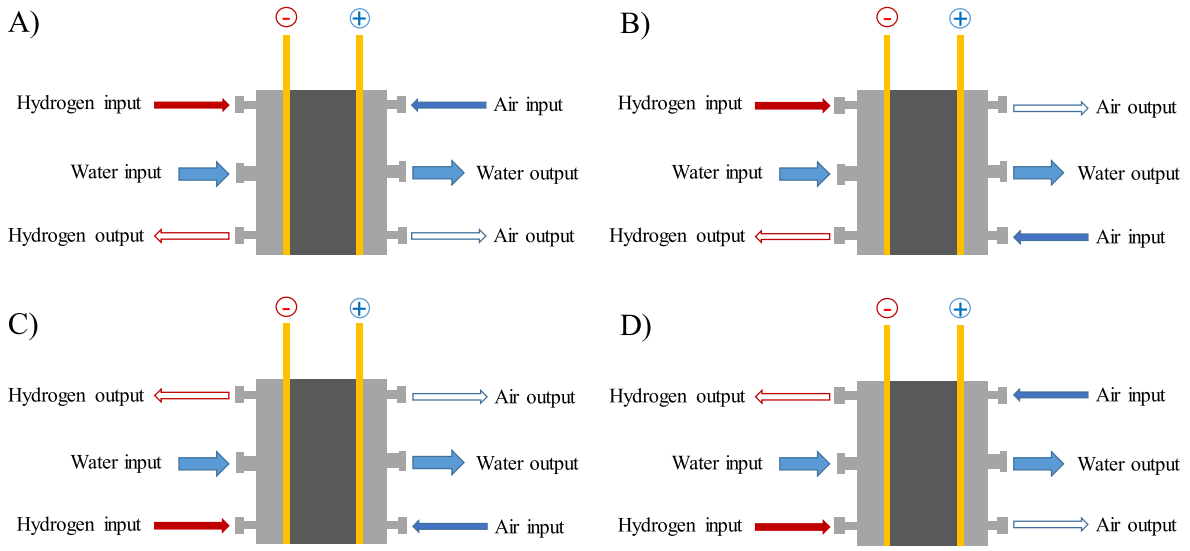

Fig. 9. Stack configurations. (A) *atct* anode and cathode gas inlet at the top and anode and cathode gas outlet at the bottom, (B) *atcb* cathode gas inlet at the bottom and cathode gas outlet at the top, (C) *abct* anode gas inlet at the bottom and anode gas outlet at the top, (D) *abcb* anode and cathode gas inlet at the bottom and anode and cathode gas outlet at the top.

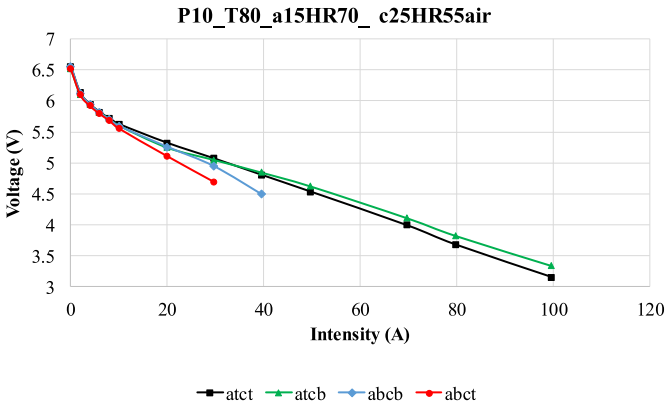

Fig. 10. Polarization curves for the change in the stack inlet/outlet flow configuration.

feeding the cathode from the bottom does not present these problems of water accumulation since the gas flow rate is sufficient to carry away the condensed water despite the negative effect of gravity. In this way, the stack benefits from a countercurrent contact arrangement of the reagents, achieving higher performance than in the base configuration. These results are consistent with the findings explained in Iranzo et al. [41].

Regarding the distribution of voltage and temperatures across the individual cells of the stack (Fig. 11 top and bottom), the results show a high level of uniformity at low current densities (Cv average of 0.5 for voltage and 0.8 for temperature at 0.06 A/cm^2, compared to 9.6 for voltage and 1.1 for temperature at 1 A/cm^2), regardless of the gas inlet/outlet configuration. The base configuration (*atct*) exhibits less voltage dispersion, despite having a greater degree of temperature dispersion. The results are also very analogous for the two configurations capable of operating at high current densities (*atct* and *atcb*), with very similar voltage distributions. However, under these operating conditions, the temperature of cells 2 has a lower and the central cell a higher temperature when air is fed through the bottom of the stack.

4. Conclusions

This study investigates the influence of various operating parameters (temperature, pressure, anode and cathode gas relative humidity and cathode stoichiometry) on the performance of each individual cell of a full PEM fuel cell stack. Different configurations of the reactants flow within the stack are also considered.

The study analyze the average stack voltage under various operating conditions and current densities. Results reveale that pressure dominates at lower current densities, while temperature becomes more influential at higher values. Kinetics significantly impacts stack performance at lower intensities, and higher pressures enhance kinetics, ultimately affecting overall cell performance. At higher current densities, increased temperature positively affects water management and promotes faster electrochemical reactions as well as enhances proton conductivity. On the other hand, when considering voltage heterogeneity, temperature is found to be the primary factor influencing voltage distribution across all current densities. Besides, as temperature non-uniformity increases, voltage non-uniformity follows suit.

The results show that the PEM fuel cell stack exhibits better performance with an increase in temperature up to 80 °C and a cathode stoichiometry of 3. In the studied range, the average cell voltage increases by around 0.07 V for every 10 °C increase at 1 A/cm^2. The operation pressure also positively affects the stack performance but to a lesser extent (voltage rises by 0.03 V for every 0.5 bar increase at 1 A/cm^2) for a high cathode stoichiometry. On the other hand, both cathode and anode relative humidity have a smaller influence on the performance, but better results have been observed at the central values, which presented 0.01V more than the extreme conditions. Therefore, the optimum operating conditions, from the stack performance point of view, are a temperature of 80 °C, an anode/cathode stoichiometry of 1.5/3, a pressure of 1 bar, and an anode/cathode relative humidity of 60/55%. It is worth noting that the voltage distribution is less uniform for operating conditions where water is susceptible to accumulation, such as high current densities (C_v 16 times higher at 1 A/cm^2 than at 0.06 A/cm^2), low temperatures (C_v 1.1 points lower at 80 °C than at 60 °C) and low cathode stoichiometry (C_v 0.6 points lower for the central condition).

Finally, gravity affects the stack performance as it hinders water evacuation from those cells where its accumulation is more persistent. Thus, feeding the reactant gases from the top of the stack is recommended even when the cell can operate slightly better (0.2 V more at 1 A/cm^2) if the air is fed from the bottom part.

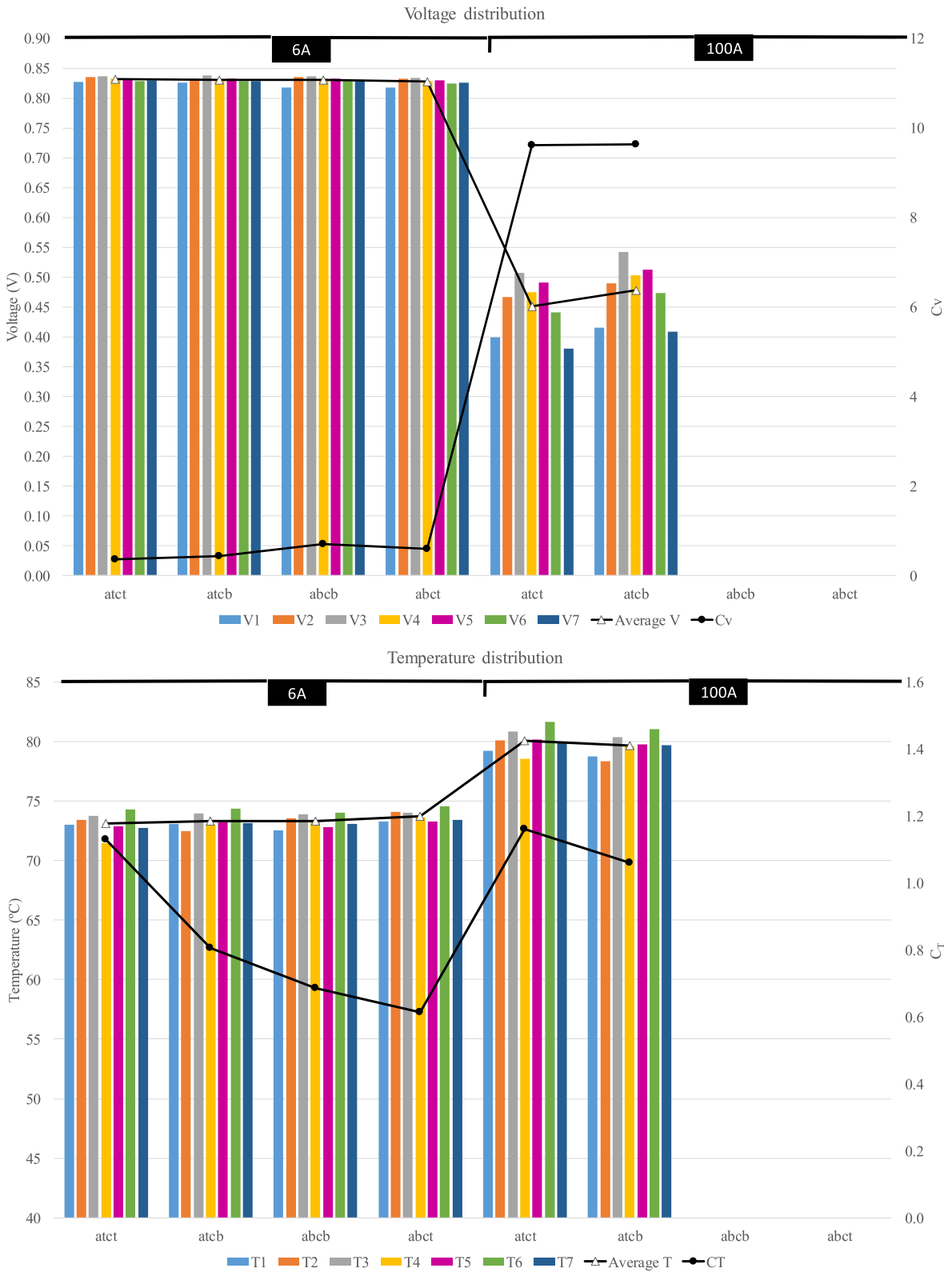

Fig. 11. Voltage (top) and temperature distribution (bottom) at a current density of 0.06 and 1 A/cm^2.

Credit author statement

G. M. Cabello González: Conceptualization; Data curation; Formal analysis; Investigation; Methodology; Validation; Visualization; Roles/Writing - original draft; Baltasar Toharias: Conceptualization; Data curation; Formal analysis; Writing - review & editing; Alfredo Iranzo: Conceptualization; Investigation; Methodology; Supervision; Validation; Visualization; Writing - review & editing; Christian Suárez: Investigation; Supervision; Writing - review & editing; Felipe Rosa: Funding acquisition; Project administration; Resources; Writing - review & editing.

Declaration of competing interest

The authors declare that they have no known competing financial interests or personal relationships that could have appeared to influence the work reported in this paper

Data availability

Data will be made available on request.

Acknowledgement

This work has been funded through Grant TED2021-130706B–I00 financed via MCIN /AEI/10.13039/501100011033 and the European Union NextGenerationEU/PRTR. Also, co-funded by Secretaría General de Universidades, Investigación y Tecnología, Plan Andaluz de Investigación, Desarrollo e Innovación (PAIDI 2020), Junta de Andalucía, with ERDF funds, grant number P20_01231. The PEM fuel cell test bench was financed by Ministerio de Ciencia e Innovación/AEI, grant number UNSE15-CE-2962, co-funded with ERDF funds.

Appendix A. Supplementary data

Supplementary data to this article can be found online at https://doi.org/10.1016/j.energy.2023.128781.

References

[1] IPCC, 2021: Climate Change 2021: The Physical Science Basis. Contribution of Working Group I to the Sixth Assessment Report of the Intergovernmental Panel on Climate Change [Masson-Delmotte, V., P. Zhai, A. Pirani, S.L. Connors, C. Péan, S. Berger, N. Caud, Y. Chen, L. Goldfarb, M.I. Gomis, M. Huang, K. Leitzell, E. Lonnoy, J.B.R. Matthews, T.K. Maycock, T. Waterfield, O. Yelekçi, R. Yu, and B. Zhou (editors)]. Cambridge University Press, Cambridge, United Kingdom and New York, NY, USA. (In press). doi:10.1017/9781009157896.

[2] El-Fergany AA, Hasanien HM, Agwa AM. Semi-empirical PEM fuel cells model using whale optimization algorithm. Energy Convers Manag 2019;201:112197. https://doi.org/10.1016/j.enconman.2019.112197.

[3] Qin Y, Liu G, Chang Y, Du Q. Modeling and design of PEM fuel cell stack based on a flow network method. Appl Therm Eng 2018;144:411–23. https://doi.org/10.1016/j.applthermaleng.2018.08.050.

[4] Maleki Bagherabadi K, Skjong S, Pedersen E. Dynamic modelling of PEM fuel cell system for simulation and sizing of marine power systems. Int J Hydrogen Energy 2022;47:17699–712. https://doi.org/10.1016/j.ijhydene.2022.03.247.

[5] Cao Y, Li Y, Zhang G, Jermsittiparsert K, Razmjooy N. Experimental modeling of PEM fuel cells using a new improved seagull optimization algorithm. Energy Rep 2019;5:1616–25. https://doi.org/10.1016/j.egyr.2019.11.013.

[6] Iranzo A, Muñoz M, Rosa F, Pino J. Numerical model for the performance prediction of a PEM fuel cell. Model results and experimental validation. Int J Hydrogen Energy 2010;35:11533–50. https://doi.org/10.1016/j.ijhydene.2010.04.129.

[7] Ogungbemi E, Wilberforce T, Ijaodola O, Thompson J, Olabi AG. Review of operating condition, design parameters and material properties for proton exchange membrane fuel cells. Int J Energy Res 2021;45:1227–45. https://doi.org/10.1002/er.5810.

[8] Iranzo A, Navas SJ, Rosa F, Berber MR. Determination of time constants of diffusion and electrochemical processes in polymer electrolyte membrane fuel cells. Energy 2021;221:119833.

[9] Saka K, Orhan MF. Analysis of stack operating conditions for a polymer electrolyte membrane fuel cell. Energy 2022;258:124858. https://doi.org/10.1016/j.energy.2022.124858.

[10] Lee J, Nguyen H-D, Escribano S, Micoud F, Rosini S, Tengattini A, et al. Neutron imaging of operando proton exchange membrane fuel cell with novel membrane. J Power Sources 2021;496:229836. https://doi.org/10.1016/j.jpowsour.2021.229836.

[11] Iranzo A, Gregorio JM, Boillat P, Rosa F. Bipolar plate research using Computational Fluid Dynamics and neutron radiography for proton exchange membrane fuel cells. Int J Hydrogen Energy 2020;45:12432–42. https://doi.org/10.1016/j.ijhydene.2020.02.183.

[12] Ijaodola OS, El- Hassan Z, Ogungbemi E, Khatib FN, Wilberforce T, Thompson J, et al. Energy efficiency improvements by investigating the water flooding management on proton exchange membrane fuel cell (PEMFC). Energy 2019;179:246–67. https://doi.org/10.1016/j.energy.2019.04.074.

[13] Shen J, Xu L, Chang H, Tu Z, Chan SH. Partial flooding and its effect on the performance of a proton exchange membrane fuel cell. Energy Convers Manag 2020;207:112537. https://doi.org/10.1016/j.enconman.2020.112537.

[14] Wang J, Geng J, Wang M, Hu X, Shao Z, Zhang H. Quantification on degradation mechanisms of polymer exchange membrane fuel cell cathode catalyst layers during bus and stationary durability test protocols. J Power Sources 2022;521:230878. https://doi.org/10.1016/j.jpowsour.2021.230878.

[15] Schmies H, Schonvogel D, Büsselmann J, Wagner P, Dyck A. Understanding degradation phenomena in {HT}-{PEM} fuel cells using micro-computed tomography. ECS Trans 2020;98:99–107. https://doi.org/10.1149/09809.0099ecst.

[16] Li B, Wan K, Xie M, Chu T, Wang X, Li X, et al. Durability degradation mechanism and consistency analysis for proton exchange membrane fuel cell stack. Appl Energy 2022;314:119020. https://doi.org/10.1016/j.apenergy.2022.119020.

[17] Miller M, Bazylak A. A review of polymer electrolyte membrane fuel cell stack testing. J Power Sources 2011;196:601–13. https://doi.org/10.1016/j.jpowsour.2010.07.072.

[18] Chen K, Hou Y, Jiang C, Pan X, Hao D. Experimental investigation on statistical characteristics of cell voltage distribution for a PEMFC stack under dynamic driving cycle. Int J Hydrogen Energy 2021;46:38469–81. https://doi.org/10.1016/j.ijhydene.2021.09.092.

[19] Hu M, Sui S, Zhu X, Yu Q, Cao G, Hong X, et al. A 10 kW class PEM fuel cell stack based on the catalyst-coated membrane (CCM) method. Int J Hydrogen Energy 2006;31:1010–8. https://doi.org/10.1016/j.ijhydene.2006.02.018.

[20] Matsushita Y, Okano J, Okajima K. Energy balance and stack performance of 1 kW class PEFC. ECS Meet Abstr 2008;MA2008–02:208. https://doi.org/10.1149/ma2008-02/1/208. –208.

[21] Jang JH, Chiu HC, Yan WM, Sun WL. Effects of operating conditions on the performances of individual cell and stack of PEM fuel cell. J Power Sources 2008;180:476–83. https://doi.org/10.1016/j.jpowsour.2008.02.001.

[22] Mehta V, Cooper JS. Review and analysis of PEM fuel cell design and manufacturing. J Power Sources 2003;114:32–53. https://doi.org/10.1016/S0378-7753(02)00542-6.

[23] Squadrito G, Barbera O, Giacoppo G, Urbani F, Passalacqua E. Polymer electrolyte fuel cell stacks at CNR-ITAE: state of the art. J Fuel Cell Sci Technol 2006;4:350–6. https://doi.org/10.1115/1.2756567.

[24] Li Y, Zhao X, Liu Z, Li Y, Chen W, Li Q. Experimental study on the voltage uniformity for dynamic loading of a PEM fuel cell stack. Int J Hydrogen Energy 2015;40:7361–9. https://doi.org/10.1016/j.ijhydene.2015.04.058.

[25] Chesalkin A, Kacor P, Moldrik P. Heat transfer optimization of NEXA ballard low-temperature PEMFC. Energies 2021;14. https://doi.org/10.3390/en14082182.

[26] Luo L, Jian Q, Huang B, Huang Z, Zhao J, Cao S. Experimental study on temperature characteristics of an air-cooled proton exchange membrane fuel cell stack. Renew Energy 2019;143:1067–78. https://doi.org/10.1016/j.renene.2019.05.085.

[27] Wang L, Quan Z, Zhao Y, Yang M, Zhang J. Experimental investigation on thermal management of proton exchange membrane fuel cell stack using micro heat pipe array. Appl Therm Eng 2022;214:118831. https://doi.org/10.1016/j.applthermaleng.2022.118831.

[28] Suárez C, Iranzo A, Toharias B, Rosa F. Experimental and numerical Investigation on the design of a bioinspired PEM fuel cell. Energy 2022:124799. https://doi.org/10.1016/j.energy.2022.124799.

[29] Xia S, Lin R, Cui X, Shan J. The application of orthogonal test method in the parameters optimization of PEMFC under steady working condition. Int J Hydrogen Energy 2016;41:11380–90. https://doi.org/10.1016/j.ijhydene.2016.04.140.

[30] Neto RC, Teixeira JC, Azevedo JLT. Thermal and electrical experimental characterisation of a 1 kW PEM fuel cell stack. Int J Hydrogen Energy 2013;38:5348–56. https://doi.org/10.1016/j.ijhydene.2013.02.025.

[31] The fuel cell testing and standarization network EU FP5 Project ENG2-CT-2002-20657. vol. 4. FCTESTNET Test procedures draft v1; 2006.

[32] FCTESTQA Test protocol. Testing the voltage and power as function of current density. Polarisation curve for a PEFC single cell. Test Module PEFC SC 5-2. European Commission, Joint Research Centre, Institute for Energy; 2010.

[33] Zhao X, Xu L, Fang C, Jiang H, Li J, Ouyang M. Study on voltage clamping and self-humidification effects of pem fuel cell system with dual recirculation based on orthogonal test method. Int J Hydrogen Energy 2018;43:16268–78. https://doi.org/10.1016/j.ijhydene.2018.06.172.

[34] Shao Y, Xu L, Hu Z, Xu L, Zhao Y, Zhao G, et al. Investigation on the performance heterogeneity within a fuel cell stack considering non-isopotential of bipolar plates. Energy 2023;263:125791. https://doi.org/10.1016/j.energy.2022.125791.

[35] Su Y, Yin C, Hua S, Wang R, Tang H. Study of cell voltage uniformity of proton exchange membrane fuel cell stack with an optimized artificial neural network model. Int J Hydrogen Energy 2022;47:29037–52. https://doi.org/10.1016/j.ijhydene.2022.06.240.

[36] Pérez-Page M, Pérez-Herranz V. Effect of the operation and humidification temperatures on the performance of a pem fuel cell stack on dead-end mode. Int J Electrochem Sci 2011;6:492–505.

[37] Chen D, Pei P, Ren P, Song X, Wang H, Zhang L, et al. Analytical methods for the effect of anode nitrogen concentration on performance and voltage consistency of proton exchange membrane fuel cell stack. Energy 2022;258:124850. https://doi.org/10.1016/j.energy.2022.124850.

[38] Salva JA, Iranzo A, Rosa F, Tapia E. Experimental validation of the polarization curve and the temperature distribution in a PEMFC stack using a one dimensional analytical model. Int J Hydrogen Energy 2016;41:20615–32. https://doi.org/10.1016/j.ijhydene.2016.09.152.

[39] Mennola T, Mikkola M, Noponen M, Hottinen T, Lund P. Measurement of ohmic voltage losses in individual cells of a PEMFC stack. J Power Sources 2002;112:261–72. https://doi.org/10.1016/S0378-7753(02)00391-9.
[40] Adzakpa KP, Ramousse J, Dubé Y, Akremi H, Agbossou K, Dostie M, et al. Transient air cooling thermal modeling of a PEM fuel cell. J Power Sources 2008;179:164–76. https://doi.org/10.1016/j.jpowsour.2007.12.102.
[41] Iranzo A, Boillat P, Biesdorf J, Tapia E, Salva A, Guerra J. Liquid water preferential accumulation in channels of PEM fuel cells with multiple serpentine flow fields. Int J Hydrogen Energy 2014;39:15687–95. https://doi.org/10.1016/j.ijhydene.2014.07.101.